3.4

Wavelet Denoising for Image Enhancement

Dong Wei
SBC Laboratories, Austin, Texas

Umesh Rajashekar and Alan C. Bovik
The University of Texas at Austin

1 Introduction

Image processing is a science that uncovers information about images. Enhancement of an image is necessary to improve appearance or to highlight some aspect of the information contained in the image. Whenever an image is converted from one form to another, e.g., acquired, copied, scanned, digitized, transmitted, displayed, printed, or compressed, many types of noise or noise-like degradations can be present in the image. For instance, when an analog image is digitized, the resulting digital image contains quantization noise; when an image is halftoned for printing, the resulting binary image contains halftoning noise; when an image is transmitted through a communication channel, the received image contains channel noise; when an image is compressed, the decompressed image contains compression errors. Hence, an important subject is the development of image enhancement algorithms that remove (smooth) noise artifacts while retaining image structure.

Digital images can be conveniently represented and manipulated as matrices containing the light intensity or color information at each spatially sampled points. The term *monochrome digital image* or simply *digital image*, refers to a two-dimensional light intensity function $f(n_1, n_2)$, where n_1 and n_2 denote spatial coordinates, the value of $f(n_1, n_2)$ is proportional to the brightness (or gray level) of the image at that point, and n_1, n_2, and $f(n_1, n_2)$ are integers.

The problem of image denoising is to recover an image $f(n_1, n_2)$ from the observation $g(n_1, n_2)$, which is distorted by noise (or noise-like degradation) $q(n_1, n_2)$; i.e.,

$$g(n_1, n_2) = f(n_1, n_2) + q(n_1, n_2). \quad (1)$$

Chapter 3.1 considers methods for linear image restoration. The classical image denoising techniques are based on *filtering*, which can be classified into two categories: *linear filtering* and *nonlinear filtering*. Linear filtering-based denoising is based on lowpass filtering to suppress high-frequency noise. The simplest lowpass filter is spatial averaging. Linear filtering can be implemented in either the spatial domain or the frequency domain (usually via fast Fourier transforms). Nonlinear filters used in denoising include order statistic filters and morphologic filters. The most popular nonlinear filter is the median filter, which is a special type of order

statistic filter. For detailed discussions of these nonlinear filters, see Chapters 3.2 (median filters), 3.3 (morphologic filters), and 4.4 (order statistic filters).

The basic difficulty with these filtering-based denoising techniques is that, if applied indiscriminately, they tend to blur the image, which is usually objectionable. In particular, one usually wants to avoid blurring sharp edges or lines that occur in the image.

Recently, wavelet-based denoising techniques have been recognized as powerful tools for denoising. Different from those filtering-based classical methods, wavelet-based methods can be viewed as transform-domain point processing.

2 Wavelet Shrinkage Denoising

2.1 The Discrete Wavelet Transform

Before introducing wavelet-based denoising techniques, we first briefly review relevant basics of the discrete wavelet transform (See Chapter 4.1 for a fuller introduction to wavelets).

The *discrete wavelet transform* (DWT) is a multiresolution (or multiscale) representation. The DWT is implemented via multirate filterbanks.

Figure 1 shows an implementation of a three-level forward DWT based on a two-channel recursive filterbank, where $h_0(n)$ and $h_1(n)$ are lowpass and highpass analysis filters, respectively, and the block $\downarrow 2$ represents the downsampling operator by a factor two. The input signal $x(n)$ is recursively decomposed into a total of four subband signals: a coarse signal $c_3(n)$ and three detail signals $d_1(n)$, $d_2(n)$, and $d_3(n)$ of three resolutions.

Figure 2 plots an implementation of a three-level inverse DWT based on a two-channel recursive filterbank, where $\tilde{h}_0(n)$ and $\tilde{h}_1(n)$ are lowpass and highpass synthesis filters, respectively, and the block $\uparrow 2$ represents the upsampling operator by a factor two. The four subband signals $c_3(n)$, $d_3(n)$, $d_2(n)$, and $d_1(n)$ are recursively combined to reconstruct the output signal $x(n)$. The four finite impulse response filters satisfy

$$h_1(n) = (-1)^n h_0(n) \tag{2}$$

$$\tilde{h}_0(n) = h_0(1-n) \tag{3}$$

$$\tilde{h}_1(n) = (-1)^n h_0(1-n) \tag{4}$$

so that the output of the inverse DWT is identical to the input of the forward DWT and the resulting DWT is an orthonormal transform.

For a signal of length N, the computational complexity of its DWT is $O(N)$, provided that the length of the filter $h_0(n)$ is negligible compared to N.

The two-dimensional (2D) DWT of a 2D signal can be implemented by using the one-dimensional (1D) DWT in a separable fashion. At each level of decomposition (or reconstruction), the 1D forward DWT (or inverse DWT) is first applied to every row of the signal and then applied to every column of the resulting data. For an image of size $N \times M$, the computational complexity of its 2D DWT is $O(NM)$, provided that the length of the filter $h_0(n)$ is negligible compared to both N and M.

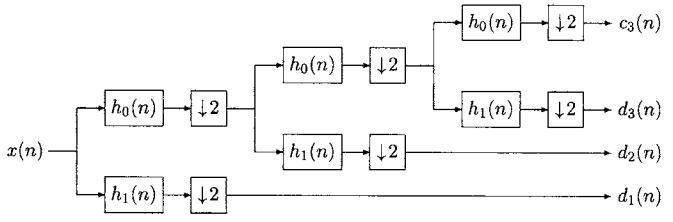

FIGURE 1 A three-level forward DWT via a two-channel iterative filterbank.

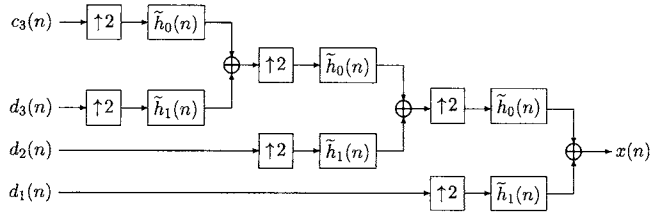

FIGURE 2 A three-level inverse DWT via a two-channel iterative filterbank.

2.2 The Donoho-Johnstone Method

The method of wavelet shrinkage denoising was developed principally by Donoho and Johnestone [1–3]. Suppose we want to recover a one-dimensional signal f from a noisy observation g; i.e.,

$$g(n) = f(n) + q(n) \tag{5}$$

for $n = 0, 1, \ldots, N-1$, where q is additive noise. The method attempts to reject noise by damping or thresholding in the wavelet domain. The estimate of the signal f is given by

$$\widehat{f} = \mathcal{W}^{-1} \mathcal{T}_\lambda \mathcal{W} g \tag{6}$$

where the operators $\mathcal{W}$ and $\mathcal{W}^{-1}$ stand for the forward and inverse discrete wavelet transforms, respectively, and $\mathcal{T}_\lambda$ is a wavelet-domain point-wise thresholding operator with a threshold λ.

The key idea of wavelet shrinkage is that the wavelet representation can separate the signal and the noise. The DWT compacts the energy of the signal into a small number of DWT coefficients having large amplitudes and spreads the energy of the noise over a large number of DWT coefficients having small amplitudes. Hence, a thresholding operation

attenuates noise energy by removing those small coefficients while maintaining signal energy by keeping these large coefficients unchanged.

There are two types of basic thresholding rules. For a given function $p(y)$, the *hard thresholding* operator is defined as

$$(\mathcal{T}_\lambda p)(y) = \begin{cases} p(y), & \text{if } |p(y)| > \lambda \\ 0, & \text{otherwise} \end{cases} \tag{7}$$

and the *soft thresholding* operator is defined as

$$(\mathcal{T}_\lambda p)(y) = \begin{cases} p(y) - \lambda, & \text{if } p(y) > \lambda \\ p(y) + \lambda, & \text{if } p(y) < -\lambda \\ 0, & \text{otherwise.} \end{cases} \tag{8}$$

Since both hard thresholding and soft thresholding are nonlinear operators, wavelet shrinkage is a type of nonlinear processing. Since $\mathcal{T}_\lambda$ is a point processing operator, its computational complexity is $O(1)$. Hence, the complexity of the DWT-based wavelet shrinkage is $O(N)$ for a length-N signal.

If the parameter λ is too large, then the thresholding operation will remove a significant amount of signal energy, i.e., it causes over-smoothing. If λ is too small, then a significant amount of noise will not be suppressed. Several approaches have been proposed for selecting the threshold λ. The simplest are *VisuShrink* [1] and *SureShrink*, which is based on *Stein's Unbiased Risk Estimate* (SURE).

Both soft thresholding and hard thresholding cause that the energy of the reconstructed signal $\hat{f}$ is lower than the energy of the noisy observation g. If an appropriate threshold is chosen, then the energy suppressed in wavelet shrinkage is mostly corresponding to the noise q. Therefore, the true signal f is not weakened after denoising.

2.3 Shift-Invariant Wavelet Shrinkage

One disadvantage of the DWT is that it is not a shift[1]-invariant transform. For instance, the DWT of $x(n-1)$ is not a shifted version of the DWT of $x(n)$. Such a shift variance is caused by the down-sampling and upsampling operations. It has been argued [4] that DWT-based wavelet shrinkage sometimes produces visual artifacts such as the "pseudo-Gibbs phenomena" in the neighborhood of discontinuities in the signal due to the lack of shift invariance of the DWT. In order to avoid the problem caused by the DWT, Coifman and Donoho and Lang et al. independently proposed to use the *undecimated DWT* (UDWT) in wavelet shrinkage to achieve shift invariance [4, 5].

[1]Since we deal with signals of finite support, by *shift* we really mean circular shift.

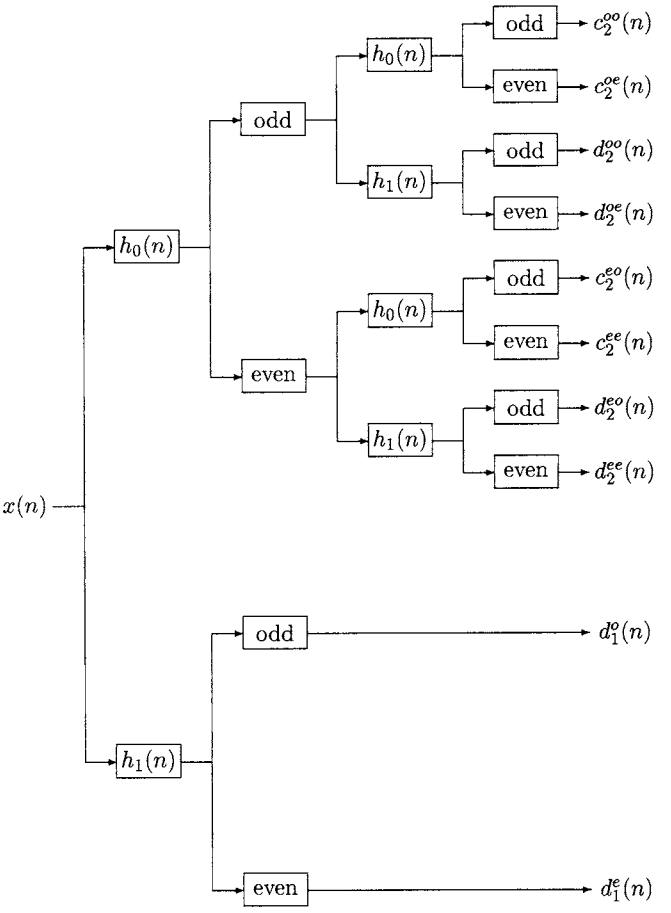

FIGURE 3 A two-level forward UDWT via a two-channel iterative filterbank. (The "odd" and "even" blocks stand for the downsamplers that sample odd-indexed and even-indexed outputs from the preceding filter, respectively.)

Figure 3 illustrates an implementation of a two-level forward UDWT based on a two-channel recursive filterbank. At each level of decomposition, both odd-indexed and even-indexed samples at the outputs of the filters $h_0(n)$ and $h_1(n)$ are maintained without decimation. Since there is no downsampler in the forward UDWT, the transform is a shift-invariant representation.

Since the number of UDWT coefficients is larger than the signal length, the inverse UDWT is not unique. In Fig. 3, if the filterbank satisfies (2), (3), and (4), then the signal $x(n)$ can be exactly reconstructed from each of the four sets of UDWT coefficients: $\{c_2^{oo}(n), d_2^{oo}(n), d_1^o(n)\}$, $\{c_2^{oe}(n), d_2^{oe}(n), d_1^o(n)\}$, $\{c_2^{eo}(n), d_2^{eo}(n), d_1^e(n)\}$, and $\{c_2^{ee}(n), d_2^{ee}(n), d_1^e(n)\}$. For denoising applications, it is appropriate to reconstruct $x(n)$ by averaging all possible reconstructions.

It has been demonstrated in [4] and [5] that the UDWT-based denoising achieves considerably better performance than the DWT-based denoising. The cost of such an improvement in performance is the increase in computational complexity. For a length-N signal, if the length of the filter $h_0(n)$ is negligible compared to N, then the computational

complexity of the UDWT is $O(N \log_2 N)$, which is higher than that of the DWT.

3 Image Enhancement via Wavelet Shrinkage

3.1 Suppression of Additive Noise

Although wavelet shrinkage was originally proposed for removing noise in 1D signals, it can be straightforwardly extended to images and other 2D signals. Replacing the 1D DWT by the 2D DWT, we can apply directly the thresholding operation on the 2D DWT coefficients. Hence, the computational complexity of the 2D DWT-based wavelet shrinkage is $O(NM)$ for an image of size $N \times M$.

The 2D version of the Donoho-Johnstone method has been extended to more sophisticated variations. Xu et al. proposed a wavelet-domain adaptive thresholding scheme to better preserve significant image features, which were identified via the spatial correlation of the wavelet coefficients at different scales [6]. Thresholding was performed only on the wavelet coefficients that do not correspond to any image features. A similar method was proposed by Hilton and Ogden in [7], where the significant wavelet coefficients were determined via recursive hypothesis tests. Malfait and Roose combined the wavelet representation and a Markov random field image model to incorporate a Bayesian statistical description for manipulating the wavelet coefficients of the noisy image [8]. Weyrich and Warhola applied the method of generalized cross validation to determine shrinkage parameters [9]. In [10], Chambolle et al. provided sharp estimates of the best wavelet shrinkage parameter in removing Gaussian noise from images.

Successful applications of denoising via wavelet shrinkage include the reduction of speckles in radar images [11] and the removal of noise in magnetic resonance imaging (MRI) data [6, 12, 13].

3.2 Removal of Blocking Artifacts in DCT-Coded Images

Lossy image coding is essential in many visual communications applications because limited transmission bandwidth or storage space often does not permit lossless image coding, where compression ratios are typically low. However, the quality of lossy-coded images can be severely degraded and unacceptable, especially at low bit rates. The distortion caused by compression usually manifests itself as various perceptually annoying artifacts. This problem calls for post-processing or enhancement of compressed images [14].

Most current image and video compression standards, such as JPEG (Chapter 5.5), H.261 (Chapter 6.1), MPEG-1, and MPEG-2 (Chapter 6.4), adopt the block discrete cosine transform (DCT). At the encoder, an image, a video frame, or a motion-compensated residual image, is first partitioned into 8×8 non-overlapping blocks of pixels. Then, an 8×8 DCT is performed on each block and the resulting transform coefficients are quantized and entropy coded. This independent processing of blocks does not take into account the between-block pixel correlations. Therefore, at low bit rates, such an encoding scheme typically leads to blocking artifacts, which manifest themselves as artificial discontinuities between adjacent blocks. In general, blocking artifacts are the most perceptually annoying distortion in images and video compressed by the various standards. The suppression of blocking artifacts has been studied as an image enhancement problem and as an image restoration problem. An overview of various approaches can be found in [14].

Though wavelet shrinkage techniques were originally proposed for the attenuation of signal-independent Gaussian noise, they work as well for the suppression of other types of distortion. In particular, wavelet shrinkage has been successful in removing coding artifacts in compressed images. Gopinath et al. first applied the Donoho-Johnstone method to attenuate blocking artifacts and obtained considerable improvement in terms of both the objective and subjective image quality [15]. The success of wavelet shrinkage in the enhancement of compressed images is a result of the *compression property* of wavelet bases [16]. In a compressed image, the remaining important features (e.g., edges) after compression are typically dominant and global, and the coding artifacts are subdominant and local (e.g., the blocking artifacts in block DCT-coded images). The wavelet transform compacts the energy of those features into a small number of wavelet coefficients having large magnitude, and spreads the energy of the coding error into a large number of wavelet coefficients having small magnitude; i.e., the image features and the coding artifacts are well-separated in the wavelet domain. Therefore, among the wavelet coefficients of a compressed image, those large coefficients very likely correspond to the original image, and those small ones very likely correspond to the coding artifacts. Naturally, keeping large coefficients and eliminating small ones (i.e., setting them to zero), or thresholding, will reduce the energy of the coding error.

Better enhancement performance can be achieved by using the UDWT-based shrinkage [17, 18] at the expense of increasing the post-processing complexity from $O(NM)$ to $O(NM\log_2(NM))$ for an $N \times M$ image. For image coding applications where fast decoding is desired, it is appropriate to use low-complexity post-processing methods. In [19], the optimal shift-invariant wavelet packet basis is searched at the encoder and the basis is used at the decoder to attenuate the coding artifacts. Such a scheme achieves comparable enhancement performance with the UDWT-based method and possesses a low post-processing complexity $O(NM)$. The expenses are two-fold: increase of encoding complexity, which is tolerable in many applications, and overhead bits required to code the optimal basis, which have a negligible effect on compression ratio.

4 Examples

In our simulations, we choose 512×512 8-bit gray-scale test images. We apply two wavelet shrinkage methods based on the DWT and the UDWT, respectively, to the distorted images and compare their enhancement performance in terms of both objective and subjective quality.

We use *peak signal-to-noise ratio* (PSNR) as the metric for objective image quality. The PSNR is defined as

$$\text{PSNR} = 10 \log_{10} \left\{ \frac{255^2}{\frac{1}{NM} \sum_{n_1=1}^{N} \sum_{n_2=1}^{M} [f(n_1, n_2) - \hat{f}(n_1, n_2)]^2} \right\} \quad (9)$$

where $f(n_1, n_2)$ and $\hat{f}(n_1, n_2)$, $1 \le n_1 \le N$, $1 \le n_2 \le M$, are the original image and the noisy image (or the enhanced image) with size $N \times M$, respectively.

We choose Daubechies' 8-tap orthonormal wavelet filter-bank for both the DWT and the UDWT [20]. We perform 5-level wavelet decomposition and reconstruction. We apply soft thresholding and hard thresholding for the DWT-based shrinkage and the UDWT-based shrinkage, respectively.

4.1 Gaussian Noise

Figure 4 illustrates an example of removing additive white Gaussian noise via wavelet shrinkage. Figure 4(a) and Fig. 4(b) display the original "Barbara" image and a noisy version, respectively. The PSNR of the noisy image is 24.6 dB. Figure 4(c) and Fig. 4(d) show the enhanced images via wavelet shrinkage based on the DWT and the UDWT, respectively. The PSNRs of the two enhanced images are 28.3 dB and 30.1 dB, respectively. Comparing the four images, we conclude that the perceptual quality of the enhanced images are significantly better than the noisy image: noise is greatly removed while sharp image features are well preserved without noticeable blurring. While both methods improve the objective and

FIGURE 4 Enhancement of a noisy "Barbara" image: (a) the original "Barbara" image; (b) image corrupted by Gaussian noise; (c) enhanced image via the DWT-based method; (d) enhanced image via the UDWT-based method.

subjective quality of the distorted image, the UDWT-based method achieves better performance, i.e., higher PSNR and better subjective quality, than the DWT-based method.

4.2 Blocking Artifacts

Figure 5 illustrates an example of suppressing blocking artifacts in JPEG-compressed images. Figure 5(a) is a part of the original "Lena" image. Figure 5(b) is the same part of a JPEG-compressed version at 0.25 bit per pixel (bpp), where blocking artifacts are clearly visible. The PSNR of the compressed image is 30.4 dB. Figure 5(c) and Fig. 5(d) are the corresponding parts in the enhanced images via the DWT-based shrinkage and the UDWT-based shrinkage, respectively. The PSNRs of the two enhanced images are 31.1 dB and 31.4 dB, respectively; i.e., the UDWT-based shrinkage achieves better objective quality. Although both of them have better visual quality than the JPEG-compressed one, the artifacts are more completely removed in Fig. 5(d) than in Fig. 5(c); i.e., the UDWT-based method achieves a better tradeoff between the suppression of coding artifacts and the preservation of image features.

5 Image Denoising Using Natural Scene Statistics

Owing to their simple, yet elegant approach to the problem of denoising, wavelet-based shrinkage schemes still remain as one of the most popular choices for denoising images. Advances in this area have led to the design of both global and spatially-adaptive local thresholds based on various optimality criteria of the denoised image. Unlike the shrinkage schemes that use a global threshold, spatially-adaptive local threshold methods vary the threshold (and hence the degree of noise suppression) based on local image structure. In general, the threshold is set to lower values around visually important image features such as edges (hence preventing any loss of image structure via thresholding), and to higher values in smoother image regions

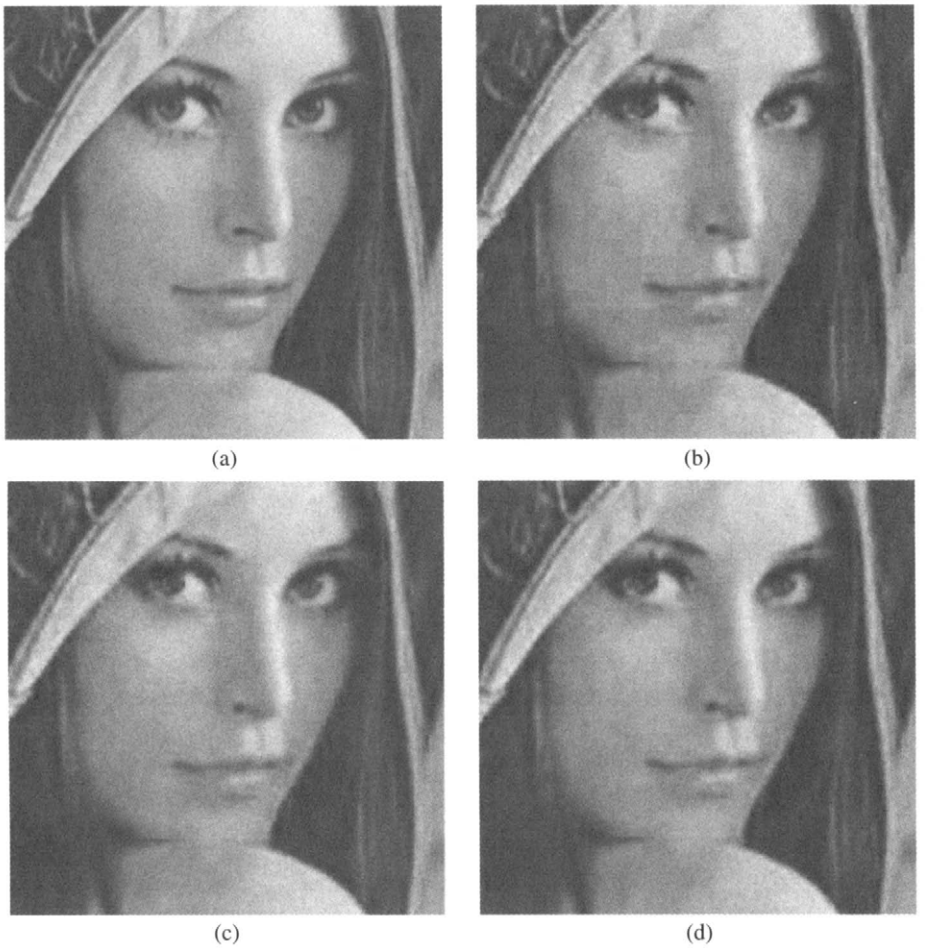

FIGURE 5 Enhancement of a JPEG-compressed "Lena" image: (a) a region of the original "Lena" image; (b) JPEG-compressed image; (c) post-processed image via the DWT-based method; (d) post-processed image via the UDWT-based method.

(thus achieving higher noise suppression) where the human visual system is sensitive to the presence of noise.

Despite their superior denoising performance, the shrinkage approaches presented above suffer from some drawbacks. The first being that wavelet coefficients that fall below the threshold are simply set to zero, irrespective of whether the coefficient was the contribution of signal or noise. Many recent approaches, instead consider image denoising simply as a flavor of signal estimation, where the goal is to *estimate* the "true" wavelet coefficient from noisy observations, based on some optimality criterion. Secondly, the shrinkage schemes are generally indifferent to the statistics of the images that are being denoised. While this generic nature of the algorithm is powerful, there is much to be gained by tuning the algorithms to the statistics of the images that are being denoised. Advances in image denoising can, therefore, greatly benefit by advances in source (in this case image statistics) modeling and is the topic of this section. In particular all the methods discussed in this section utilize a priori stochastic models to capture *statistical regularities of wavelet coefficients* for denoising natural images that have been corrupted by additive white Gaussian noise.

Modeling statistical regularities in natural images has been an active area of research in neuroscience for many years, where scientists have used inferences from natural scene statistics (NSS) to indirectly investigate and model different aspects of the human visual system (HVS). Since the HVS evolved in a natural environment, and natural images occupy a relatively small subspace of all possible images, it is theorized that the neural circuitry in the HVS exploits these statistical redundancies to represent its input efficiently [21, 22]. Based on this assumption of efficient representation, researchers analyzed patches of natural images using transforms such as principal component analysis and the more recent independent component analysis, and discovered that the resulting image basis functions indeed resemble certain cortical receptive fields [23, 24]. The reader is directed to [22] for an overview of recent advances of NSS and its relationships to neural representations. Also, Chapter 4.7 in this *Handbook* provides an overview of different models for NSS. Since the end-receiver of most images is the human eye, these powerful discoveries seem to indicate that there is much to be gained by incorporating NSS in the design of image processing algorithms. As we will see shortly, stochastic models of wavelet coefficients, though empirical, have great potential in image processing applications such as denoising.

5.1 Denoising Using Models for Marginal Distributions of Wavelet Coefficients

While there are many models that capture statistical redundancies in natural scenes (see Chapter 4.7 in this *Handbook*), we will present a model of NSS that is directly relevant to the problem of image denosing in the wavelet domain. Early stochastic models for wavelet coefficients were driven by empirical modeling of the marginal distributions of wavelet coefficients (except for the low-pass residual) as a subband-dependent mixture of independent, parameterized generalized Gaussian distributions of the form $p_Y(y) = Ke^{-(|y|/\alpha)^\beta}$, where β and α are the shape and variance parameters respectively of the probability distribution function $p_Y(y)$, and K is a scaling factor [25]. Other stochastic models represent these marginal distributions as conditionally independent zero-mean Gaussian random variables given their variances [26]. This empirical model is motivated by the observation that when the leptokurtotic marginal distributions of wavelet coefficients of natural images in a subband are normalized by their local standard deviations, the normalized histogram is well approximated by a zero-mean, unit-variance Gaussian probability density function.

Let us assume that an image is corrupted by additive white Gaussian noise and that we use an orthonormal wavelet family for analysis. Given a noisy observation of a wavelet coefficient $Y(k) = X(k) + n(k)$, the goal of image denoising in the wavelet domain is to estimate $X(k)$, where n is the white Gaussian noise with a known variance σ_n^2, and $X(k)$ is a wavelet coefficient in the uncorrupted image. The conditional Gaussian assumption of the marginal distribution of the wavelet coefficients described earlier lends this estimation to elegant mathematic formulation [26]. If the variance $\sigma^2(k)$ of $X(k)$ is known, the wavelet coefficients $X(k)$ are independent Gaussian random variables and the minimum mean square estimate (MMSE) $\hat{X}(k)$ of $X(k)$ can be shown to be simply the local Wiener-like estimate $\hat{X}(k) = \frac{\sigma^2(k)}{\sigma^2(k)+\sigma_n^2} Y(k)$.

However, in order to use this approach for image denoising, the hidden variance parameter $\sigma^2(k)$ must be computed before $\hat{X}(k)$ can be estimated. The general approach for determining this hidden variance field is to build an estimate for it by an observation of the noisy wavelet coefficients in a neighborhood surrounding $Y(k)$. In one approach [26], using the maximum likelihood (ML) framework, the authors estimated the hidden variance of each co-efficient by $\sigma^2(k) = \frac{1}{M}\sum_{j\in N(k)}(Y^2(j) - \sigma_n^2)$, where $N(k)$ is a neighborhood (of size M) of wavelet coefficients surrounding $Y(k)$. As an extension, based on empirical observations, the authors assumed exponential prior distributions of the hidden variance field for each subband, and derived the maximum a posteriori (MAP) estimate for the variance field. Using these methods to denoise images in the wavelet domain, the authors report a gain of 2 dB to 4 dB in PSNR over the hard-thresholding method and about 2 dB to 3 dB gain over the spatially optimal, minimum-mean-square-error (MMSE), local Wiener filtering.

These models for the marginals of wavelet coefficients of natural scenes have also been used in the design of spatially adaptive thresholds for denoising in the wavelet domain. Note that in the previous approach, $\sigma^2(k)$ was evaluated from just a local neighborhood, and can therefore result in noisy

estimates. To alleviate this effect, Chang et al. [27] developed a spatially adaptive thresholding scheme where the threshold was selected to be inversely proportional to the hidden variance parameter. Such a threshold selection is shown to be close to the optimal threshold which minimizes the mean square error of the soft-thresholding estimator. Instead of estimating $\sigma^2(k)$ using only a small neighborhood around the wavelet coefficient, the method of *context-modeling* was used to characterize the *context* or *activity* of a particular wavelet coefficient based on a weighted average of the absolute value of its neighbors. To estimate $\sigma^2(k)$ for a wavelet coefficient, all coefficients with a context variable similar to the coefficient under consideration were grouped together and the variance parameter estimated from this cluster using maximum likelihood estimation. Note that this variance estimate is not a function of simply the neighbors in a local neighborhood, but can contain coefficients from anywhere in the subband, as long as they have the same context. Using this scheme in an over-complete wavelet representation, the authors demonstrated an improvement of around 1 dB PSNR gain over the previous method.

5.2 Denoising Using the Gaussian Scale Mixture Model for Wavelet Coefficients

The model for NSS used above is somewhat limited since it attempts to capture only the marginal distributions of wavelet coefficients in a particular subband. Even though the wavelet coefficients are decorrelated, they are not statistically independent—there clearly exist many strong statistical relationships between the magnitude of the wavelet coefficients, both within and across subbands. For example, coefficients of large magnitudes tend to cluster together in the same subband and at similar spatial locations at other scales. In fact, zerotree-based image coders exploit this redundancy in space and scale to achieve higher compression. As another example of these robust statistical regularities, it has been found that the variance of a child wavelet coefficient in natural images is proportional to the magnitude of its parent [28]. The reader is directed to Chapter 4.7 in this *Handbook* for a more detailed description and examples that illustrate these dependencies of wavelet coefficients.

To account for these *joint* relationships, Wainwright et al. [29] proposed the Gaussian scale mixture (GSM) model to capture both the marginal and the joint distributions of the wavelet coefficients across subbands. Briefly, a random vector, X, is a GSM if and only if it can be decomposed into a product of two random variables, i.e., $X = \sqrt{z}U$, where U is a zero-mean, Gaussian random vector with covariance matrix C_u, and z is an independent positive scalar random variable. Note that if z is known, the distribution of X is Gaussian, and hence the marginal distributions are captured. The covariance matrix C_u used in the model accounts for the joint distributions of coefficients in a local neighborhood (which can include coefficients from other subbands). The reader is directed to Chapter 4.7 for a more detailed description of this model.

This GSM model of wavelet coefficients in a local neighborhood has proved to be very effective in denoising images corrupted by AWGN. Following an estimation of the signal covariance matrix C_u from a local neighborhood of wavelet coefficients, authors have derived both ML [30] and MAP (assuming a log-normal prior on z) [31] estimates of the hidden variance field. The denoised wavelet coefficient is then estimated using a local Wiener-like estimator as before. Recently, a one-step, optimal local Bayesian least squares (BLS) solution was proposed for denoising natural images corrupted by AWGN [32]. This technique obviates the need to first estimate the hidden variance field from local observations and then perform the Wiener estimation. The BLS-GSM model is shown to outperform other state-of-the-art image denoising schemes. An example of the BLS-GSM denoising scheme is shown in Chapter 4.7 in this *Handbook*.

In conclusion, incorporating models of natural scene statistics does provide significant PSNR gains over traditional wavelet-based shrinkage algorithms. Although this section focused strictly on the statistics of natural scenes, the framework easily extends to other synthetic or non-natural images such as x-rays, fMRI, and synthetic aperture radar images, provided their statistics can be captured effectively.

6 Summary

We have presented an overview of image enhancement via wavelet denoising. Compared to many classical filtering-based methods, wavelet-based methods can achieve a better tradeoff between noise reduction and feature preservation. Another advantage of wavelet denoising is its low computational complexity. Wavelet denoising is a powerful tool for image enhancement. The success of wavelet image denoising derives from the same property as does the success of wavelet image compression algorithms (Chapter 5.4): the compact image representation provided by the discrete wavelet transform.

References

[1] D. L. Donoho and I. M. Johnstone. Ideal spatial adaptation via wavelet shrinkage. *Biometrika*, 81:425–455, 1994.

[2] D. L. Donoho. De-noising by soft-thresholding. *IEEE Trans. Inform. Theory*, 41(3):613–627, May 1995.

[3] D. L. Donoho and I. M. Johnstone. Adaptation to unknown smoothness via wavelet shrinkage. *J. Amer. Stat. Assoc.*, 90:1200–1224, 1995.

[4] R. R. Coifman and D. L. Donoho. Translation-invariant de-noising. In A. Antoniadis and G. Oppenheim, editors, *Wavelets and Statistics*, 125–150. Springer, Berlin, Germany, 1995.

[5] M. Lang, H. Guo, J. E. Odegard, C. S. Burrus, and R. O. Wells Jr. Noise reduction using an undecimated discrete wavelet transform. *IEEE Signal Processing Letters*, 3(1):10–12, January 1996.

[6] Y. Xu, J. B. Weaver, D. M. Healy, Jr., and J. Lu. Wavelet transform domain filters: A spatially selective noise filtration technique. *IEEE Trans. Image Processing*, 3(6):747–758, November 1994.

[7] M. L. Hilton and R. T. Ogden. Data analytic wavelet threshold selection in 2D signal denoising. *IEEE Trans. Signal Processing*, 45(2):496–500, February 1997.

[8] M. Malfait and D. Roose. Wavelet-based image denoising using a markov random field *a priori* model. *IEEE Trans. Image Processing*, 6(4):549–565, April 1997.

[9] N. Weyrich and G. T. Warhola. Wavelet shrinkage and generalized validation for image denoising. *IEEE Trans. Image Processing*, 7(1):82–90, January 1998.

[10] A. Chambolle, R. A. DeVore, N. Lee, and B. J. Lucier. Nonlinear wavelet image processing: Variational problems, compression, and noise removal through wavelet shrinkage. *IEEE Trans. Image Processing*, 7(3):319–335, March 1998.

[11] P. Moulin. A wavelet regularization method for diffuse radar-target imaging and speckle-noise reduction. *J. Math. Imaging Vision*, 3(1):123–134, January 1993.

[12] J. B. Weaver, Y. Xu, D. M. Healy, Jr., and L. D. Cromwell. Filtering noise from images with wavelet transforms. *Magn. Reson. Med.*, 21(2):288–295, 1991.

[13] M. L. Hilton, T. Ogden, D. Hattery, G. Eden, and B. Jawerth. Wavelet denoising of functional MRI data. In A. Aldroubi and M. Unser, editors, *Wavelets in Medicine and Biology*, 93–114. CRC Press, Boca Raton, FL, 1996.

[14] M.-Y. Shen and C.-C. J. Kuo. Review of postprocessing techniques for compression artifact removal. *J. Visual Commun. Image Represen.*, 9(4):2–14, March 1998. Special Issue on High-Fidelity Media Processing.

[15] R. A. Gopinath, M. Lang, H. Guo, and J. E. Odegard. Wavelet-based post-processing of low bit rate transform coded images. In *Proc. IEEE Int. Conf. Image Processing*, volume II, 913–917, Austin, TX, November 1994.

[16] D. L. Donoho. Unconditional bases are optimal bases for data compression and for statistical estimation. *Appl. Comput. Harmon. Anal.*, 1(1):100–115, December 1993.

[17] D. Wei and C. S. Burrus. Optimal wavelet thresholding for various coding schemes. In *Proc. IEEE Int. Conf. Image Processing*, volume I, 610–613, Washington, DC, October 1995.

[18] Z. Xiong, M. T. Orchard, and Y.-Q. Zhang. A deblocking algorithm for JPEG compressed images using overcomplete wavelet representations. *IEEE Trans. Circuits Syst. Video Tech.*, 7(2):433–437, April 1997.

[19] D. Wei and A. C. Bovik. Enhancement of compressed images by optimal shift-invariant wavelet packet basis. *J. Visual Commun. Image Represen.*, 9(4):15–24, March 1998. Special Issue on High-Fidelity Media Processing.

[20] I. Daubechies. *Ten Lectures on Wavelets.* Soc. Indus. Appl. Math., Philadelphia, PA, 1992.

[21] H. B. Barlow. Possible principles underlying the transformation of sensory messages. Cambridge MA: M.I.T. Press, 217–234, 1961.

[22] E. P. Simoncelli, and B. A. Olshausen. Natural image statistics and neural representation *Annual Review of Neuroscience*, 24:1193–1216, May 2001

[23] P. J. B. Hancock, R. J. Baddeley, and L. S. Smith. The principal components of natural images *Network*, vol. 3, 61–70, 1992.

[24] J. H. van Hateren and A. van der Schaaf. Independent component filters of natural images compared with simple cells in primary visual cortex. *Proc. R. Soc. Lond.* vol. B 265, 359–366, 1998

[25] Mallat, S. G. A theory for multiresolution signal decomposition: the wavelet representation. *IEEE Tran. on Pattern Analysis and Machine Intelligence*, 11(7):674–693, July 1989.

[26] M. K. Mihcak, I. Kozintsev, K. Ramchandran, and P. Moulin, Low-complexity image denoising based on statistical modeling of wavelet coefficients. *IEEE Signal Processing Letters*, 6(12): 300–303, Dec. 1999.

[27] S. G. Chang, Bin Yu, and M. Vetterli Spatially adaptive wavelet thresholding with context modeling for image denoising. *IEEE Trans. Image Processing*, 9(9):1522–1531, Sept. 2000.

[28] E. P. Simoncelli. Statistical models for images: Compression, restoration and synthesis. *Proc. of 31st Asilomar Conference on Signals, Systems and Computers*, Pacific Grove, CA. November 2–5, 1997.

[29] M. J. Wainwright, and E. P. Simoncelli. Scale mixtures of Gaussians and the statistics of natural images. *Adv. Neural Information Processing Systems (NIPS* 1999)*, v12, May 2000.

[30] V. Strela, J. Portilla, and E. P. Simoncelli. Image denoising using a local Gaussian scale mixture model in the wavelet domain. *Proc. SPIE 45th Annual Meeting*, San Diego, CA, July 2000.

[31] J. Portilla, V. Strela, M. Wainwright, and E. P. Simoncelli. Adaptive Wiener denoising using a Gaussian scale mixture model in the wavelet domain. *Proc. 8th IEEE Int'l Conf. on Image Processing*, Thessaloniki, Greece, Oct 2001.

[32] J. Portilla, V. Strela, M. J. Wainwright, and E. P. Simoncelli. Image Denoising using Scale Mixtures of Gaussians in the Wavelet Domain. *IEEE Trans. Image Processing*, 12(11): 1338–1351, Nov 2003.